Engineering and Applied Sciences
2023; 8(1): 5-15
http://www.sciencepublishinggroup.com/j/eas
doi: 10.11648/j.eas.20230801.12
ISSN: 2575-2022 (Print); ISSN: 2575-1468 (Online)

Development of Bi-Stable Vibration Energy Harvesting System Using Duffing-Type Motion Model

Xuguang Zhang[1], Wei Zhao[2], Jingchao Guan[1], Apollo B. Fukuchi[1], Xilu Zhao[1, *]

[1]Department of Mechanical Engineering, Saitama Institute of Technology, Saitama, Japan

[2]Space C5 Co., Ltd., Tokyo, Japan

Email address:

zxg@live.jp (Xuguang Zhang), shunsuke0390@gmail.com (Wei Zhao), guanjingchao123@gmail.com (Jingchao Guan), apollo-fukuchi@sit.ac.jp@sit.ac.jp (Apollo B. Fukuchi), zhaoxilu@sit.ac.jp (Xilu Zhao)

[*]Corresponding author

To cite this article:

Xuguang Zhang, Wei Zhao, Jingchao Guan, Apollo B. Fukuchi, Xilu Zhao. Development of Bi-Stable Vibration Energy Harvesting System Using Duffing-Type Motion Model. *Engineering and Applied Sciences*. Vol. 8, No. 1, 2023, pp. 5-15. doi: 10.11648/j.eas.20230801.12

Received: February 21, 2023; **Accepted**: March 8, 2023; **Published**: March 21, 2023

Abstract: Vibration power generation is an important issue in development of renewable energy. If a vibration system with a maximum possible amplitude is designed, it can be advantageous in improving the vibration power generation efficiency. In this study, we propose a Duffing-type bi-stable vibration energy harvesting system that utilizes the stochastic resonance phenomenon, which can significantly expand the vibration amplitude. We designed the motion rail shape of the bistable vibration model using the Duffing function, and created a Duffing-type wave-shaped motion rail using an acrylic plate. An electromagnetic motor was installed in place of the four rotating wheels below the mass block that moves on the wave-shaped motion rail. When the mass block moves on the rail, it can output a voltage directly from the electromagnetic motor. To verify the performance of the proposed bi-stable vibration energy-harvesting system, a vibration experiment was conducted by combining a random excitation signal that simulates an actual natural environment and intentional periodic excitation signal. Using the experimental results, the stochastic resonance phenomenon and vibration power generation performance of the bi-stable vibration energy-harvesting system were investigated. The stochastic resonance phenomenon can be reliably generated using the bi-stable vibration system proposed in this study, and a large amplitude expansion effect can be obtained in the response vibration of the mass block. In addition, using random signals simulating the natural environment and periodic signals as stimulus signals, vibration experiments were conducted separately for two measurement cases: single excitation and joint excitation. The measurement results showed that under the same input excitation energy, the simultaneous excitation of the two signals generated 82.99% more power than that generated by separate excitation of the two signals. The generation of the stochastic resonance phenomenon by exciting two signals simultaneously has a significant effect on the improvement of the power generation efficiency of the bi-stable vibration energy harvesting system.

Keywords: Bi-Stable Vibration System, Duffing Moving Model, Vibration Energy Harvesting, Stochastic Resonance, Vibration Measurement Experiment, Vibration Power Generation

1. Introduction

The generation of vibration power from renewable energy is an important research topic. In a vibration power generation system, a relatively large amount of vibration power can be generated by increasing the response vibration amplitude as much as possible [1-5].

To increase the response vibration amplitude of the vibrating body, it is important to design the natural frequency of the vibration power generation system such that it matches the excitation frequency of the vibrating environment, and many studies regarding this have been published [6-9]. However, there are only a few vibration sources with simple frequencies in the natural environment, and application of this method is practically impossible.

To address this problem, methods of assembling vibration models with different natural frequencies into a single vibration power generation system have been investigated [10-13]. Methods for introducing nonlinear stiffness or

nonlinear restoring force into vibration systems have also been investigated [14-19]. Vibration systems with more complex geometries or systems combining multiple vibration power generation methods have been studied [20-25]. However, because of the relatively small vibration amplitudes considered in these studies, none of the research results have been applied practically.

Therefore, research and development on vibration energy harvesting using the stochastic resonance phenomenon, that can significantly expand the vibration amplitude, has attracted considerable attention [26, 27]. Stochastic resonance is a physical phenomenon in which the response signal is significantly amplified under a certain probability by adding a periodic signal to a bi-stable system, which receives random noise signals [28].

To generate stochastic resonance in a mechanical system, three conditions are necessary: a bi-stable vibration system, random noise input signal, and periodic input signal. Among these, developing a bi-stable vibration system is most important.

Among the bi-stable oscillatory systems in previous studies, a cantilever beam with a mass block at the tip is the most commonly used system with two representative types [29, 30]. One uses the opposing repulsive force between permanent magnets attached to the tip of the cantilever and attached to a nearby fixed wall [31-35]. The other uses the elasticity of bending the cantilever to the side by the gravity of the mass block attached to the tip of the inverted cantilever [36-38].

The amplitude of the cantilever beam was relatively small, and it vibrated while being bent significantly. However, the vibration continuing in a state close to buckling is a problem. Therefore, the authors proposed a new bi-stable vibration model composed of elastic springs and a mass block supported from the diagonal direction, and proposed a horizontal large-scale bi-stable vibration model [39-42].

However, the conventional bi-stable vibration model consisting of elastic springs and mass blocks is limited by configuration conditions such as the effective length of the elastic springs. Therefore, to improve the efficiency of the vibration power generation, a new bi-stable vibration model must be proposed and studied.

In this study, we directly used the potential energy distribution function of the Duffing equation of motion to design a wave-shaped rail for a new bi-stable vibration model. A duffing-wave-shaped rail was created using an acrylic plate. Four electromagnetic motors were mounted below a mass block that was moved on a wave-shaped rail. When the mass block moves on the wave-shaped rail, it can output a voltage directly from the electromagnetic motors. Therefore, a nonlinear equation of motion for a bi-stable oscillatory system was created. The bi-stable vibration characteristics of the developed vibration system were theoretically analyzed. The experimental equipment was developed, and vibration experiments were performed using a shaking table. The amplification effect and power generation characteristics of the proposed bi-stable vibration power generation system were verified.

2. Materials and Methods

2.1. Bi-Stable Vibration Model

Figure 1 shows a vibration model consisting of an arc-shaped rail and mass block. R is the radius of curvature of the arc-shaped rail, m is the mass of the moving mass block, and $\ddot{x}_e$ is the excitation acceleration of the arc-shaped rail. As shown in Figure 1, when the arc-shaped rail vibrates from the outside, the equation of motion for the relative displacement of the mass block with respect to the arc-shaped rail along the x-direction is expressed by the following equation:

$$m\ddot{x} + \frac{mg}{R}x = m\ddot{x}_e \tag{1}$$

A graph of the potential energy of the vibration model of Figure 1 is shown in Figure 2.

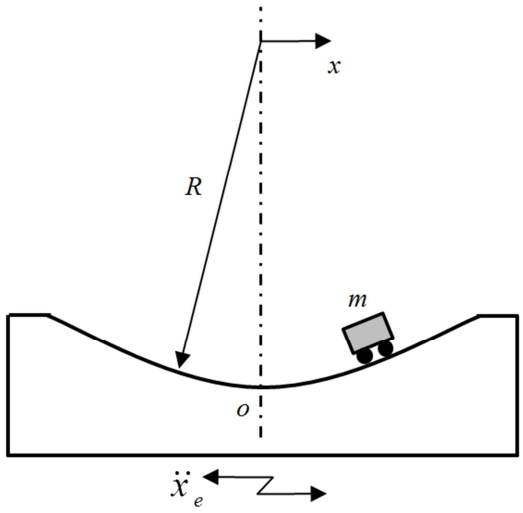

Figure 1. *Sample of Single stable vibration model.*

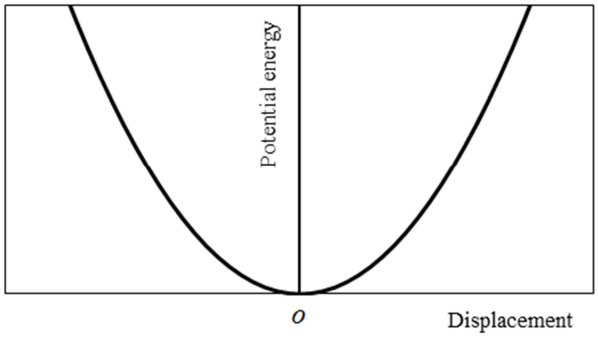

Figure 2. *Potential energy distribution of mono-stable vibration model.*

As seen in Figures 1 and 2, midpoint o of the arc-shaped rail corresponds to the lowest point of the potential energy and also the stable position of the mass block at rest. The mass block vibrates around the stable position o by excitation of the arc-shaped rail, and such a vibrating state is called mono-stable vibration.

However, instead of an arc-shaped rail, the vibration model is composed of a wave-shaped rail and a mass block, as shown in Figure 3. At the midpoint of the corrugated rail, there is a local vertex o, and on either side, are two local stable points a_1 and a_2.

When the wave-shaped rail vibrates with a small amplitude, the mass block undergoes mono-stable vibration about the left stable point a_1 or right stable point a_2. Conversely, when the wave-shaped rail vibrates with a relatively large amplitude, the mass block goes over the central vertex o and vibrates across the two stable points a_1 and a_2 on both sides; such a vibrating state is called bi-stable vibration.

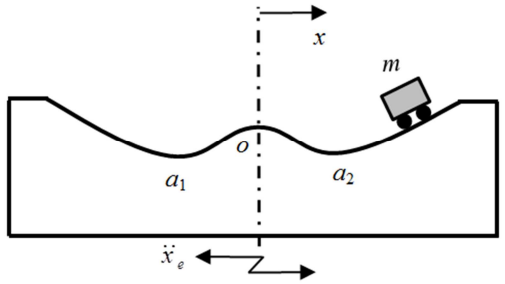

Figure 3. *Sample of bi-stable vibration model.*

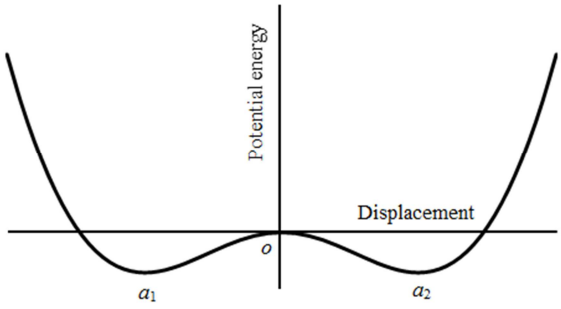

Figure 4. *Potential energy distribution of bi-stable vibration model.*

The wave-shaped rail shown in Figure 3 can be represented using the Duffing function [29].

$$y = -\frac{a}{2}x^2 + \frac{b}{4}x^4 \tag{2}$$

For confirmation, a = 2 and b = 0.25, are substituted into equation (2), and the obtained function graph is shown in Figure 5.

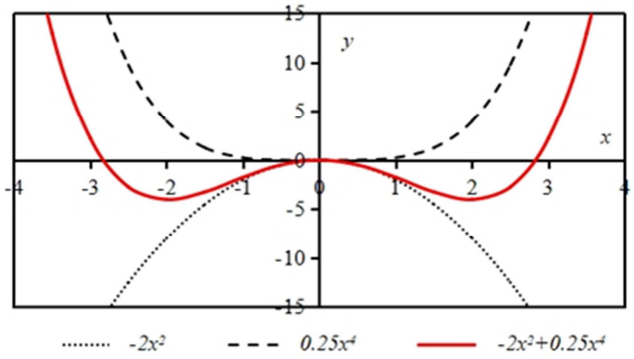

Figure 5. *Constructing a bi-stable function.*

In Figure 5, the dotted and dashed lines indicate the quadratic and quartic functions, respectively. As shown by the solid red line, which is the sum of the quartic and quadratic function, it matches the potential energy function of the bi-stable oscillation in Figure 4.

2.2. Bi-Stable Vibration Energy Harvesting System

Figure 6 shows the experimental setup of the bi-stable vibration energy harvesting system. As shown in Figure 6, the experimental setup consists of two parts: a transparent acrylic wave-shaped rail and moving mass block.

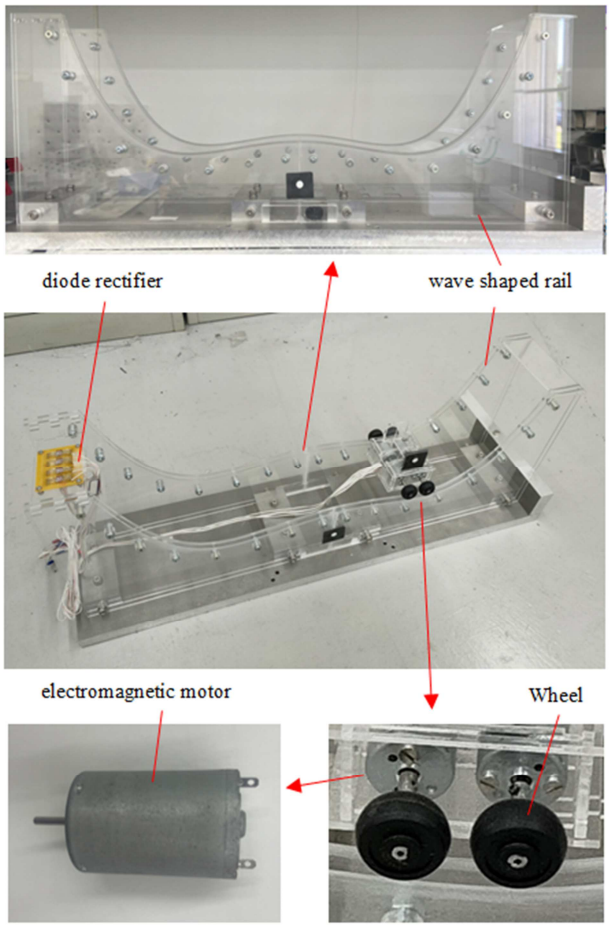

Figure 6. *Bi-stable vibration power generation experimental device.*

However, the wave-shaped rail uses the shape of the Duffing function shown in Equation (2). Four rubber foils are attached to each side of the moving mass block. An electromagnetic motor is attached to each rotating wheel.

When the wave-shaped rail vibrates in the horizontal direction, the mass block reciprocates. At that time, the rotating shaft of the electromagnetic motor rotates together with the rubber foil such that an alternating voltage can be output from the lead wires of the electromagnetic motor.

However, to prevent the phenomenon of canceling out the simultaneous voltage output from the four electromagnetic motors, the AC voltage signal output from the electromagnetic motors is passed through a diode rectifier circuit, as shown in Figure 6. It converts the AC voltage to DC and outputs it.

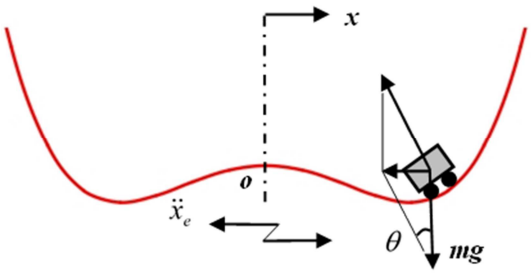

Figure 7. *Force conditions for bi-stable vibration model.*

The moving part of the experimental setup of the bistable vibration energy harvesting system shown in Figure 6 is removed, and its schematic is shown in Figure 7.

According to Figure 7, the equation of motion for the relative displacement of the mass block with respect to the wave-shaped rail along the x-direction is given by the following equation:

$$m\ddot{x} + c\dot{x} + mg\tan\theta = m\ddot{x}_e \tag{3}$$

where m is the mass of the moving mass block, c is the damping coefficient owing to friction, and $\ddot{x}_e$ is the excitation acceleration.

As the shape of the wave-shaped rail shown in Figure 7 is represented by the Duffing function of Equation (2), the angle during movement is represented by the following equation:

$$\tan\theta = \frac{d}{dx}\left(-\frac{a}{2}x^2 + \frac{b}{4}x^4\right) = -ax + bx^3 \tag{4}$$

Substituting equation (4) into equation (3), the equation of motion is expressed as follows:

$$m\ddot{x} + c\dot{x} + mg(-ax + x^3) = m\ddot{x}_e \tag{5}$$

Equation (5) shows that the bistable equation of motion shown in Figure 6 is nonlinear. Furthermore, from equation (5), the potential energy of the bistable motion system shown in Figure 6 is obtained using the following equation:

$$U = mg(-\frac{a}{2}x^2 + \frac{b}{4}x^4) \tag{6}$$

As equation (6) matches equation (2), the bistable motion system shown in Figure 6 is a Duffing-type motion system. Furthermore, to analyze the potential energy distribution of the bistable motion system using equation (6), we solve the following equation obtained from differentiation with respect to equation (6):

$$\frac{dU}{dx} = -ax + bx^3 = 0 \tag{7}$$

By solving the cubic equation (7), three solutions are obtained, as shown below.

$$x_1 = -\sqrt{\frac{a}{b}} \quad x_2 = 0 \quad x_3 = \sqrt{\frac{a}{b}} \tag{8}$$

The three values shown in equation (8) correspond to the local extreme values a_1, o, and a_2 of the potential energy of the bistable vibration model shown in Figure 4. The difference between the local maximum and minimum values of potential energy can be calculated using the following equation:

$$\Delta U = U(x_1) - U(x_2) = mg\frac{a^2}{4b} \tag{9}$$

The value of equation (9) indicates the barrier value ΔU of the energy required for the moving mass block to cross over the center point from the left or right stable point and generate a bistable vibration.

When applying the bistable vibration power generation system shown in Figure 6, the moving mass block is designed to perform monostable vibration on the left or right side of the wave-shaped rail according to the random excitation intensity in the natural world.

To improve the power generation efficiency of the vibration energy harvesting system, an appropriate periodic signal was simultaneously applied as a stimulus signal to the vibration system under random vibration. Therefore, through application of a weak periodic signal, the vibration state of the mass block changed from a mono-stable to bistable vibration over the central peak, and the vibration amplitude increased significantly. This phenomenon is known as the stochastic resonance.

This research aims at elucidating the large amplification effect that can be obtained when the mass block exceeds the peak of the potential energy at the center when stochastic resonance occurs, and also utilize it to improve the efficiency of vibration power generation.

2.3. Vibration Experiment System

Figure 8 shows the experimental apparatus developed for bistable vibration energy harvesting. Figure 9 shows the flow chart of the measurement experiment and signal flow, where the vibration signals and measurement results are indicated by arrows and square brackets, respectively.

As shown in Figures 8 and 9, when performing the vibration experiments, random and periodic signals generated from signal generators A and B, respectively, are sent to a two-channel amplifier and amplified. The amplified random and periodic signals were then sent to a general shaker and mini-shaker, respectively. The electromagnetic motor generates vibration power by vibrating a bi-stable vibration power generator.

Furthermore, to measure the experimental results of the relative vibration displacement between the moving mass block and wave-shaped rail, measurement markers were attached to the surfaces of the moving mass block and wave-shaped rail. During the measurement experiment, a high-speed video camera was used to record motion videos of the measurement markers. After the measurement experiment was completed, the movement video of the measurement marker was read into a personal computer, and the time-displacement data of the measurement marker were

obtained by performing processing of tracking using tracking software.

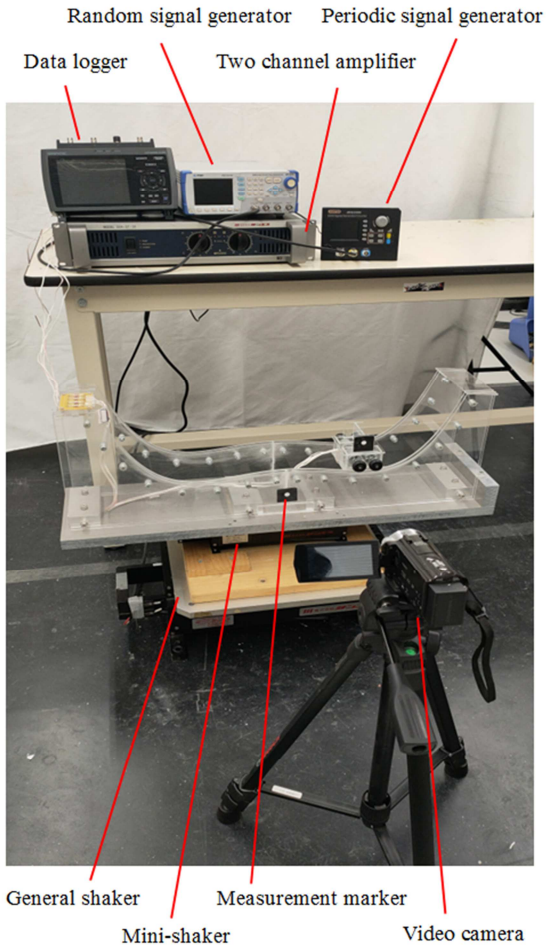

Figure 8. *Bi-stable vibration energy harvesting experimental system.*

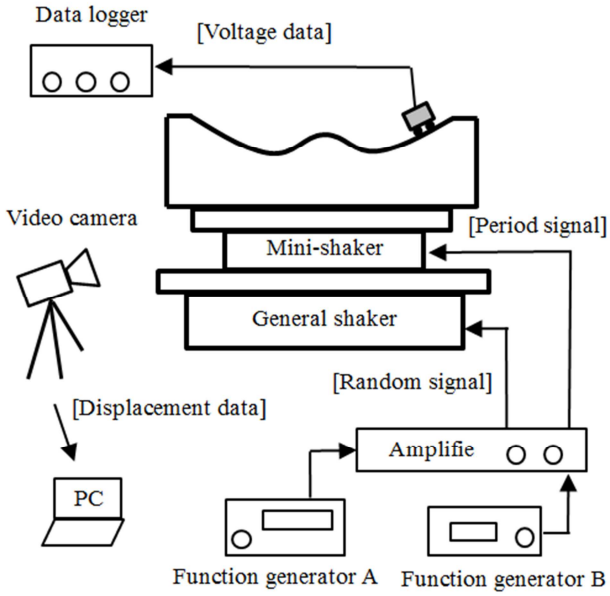

Figure 9. *Measurement experiment flow chart and signal flow.*

On the other hand, to measure the experimental results of vibration power generation, the AC voltage signals output from the four electromagnetic motors were converted into DC voltage signals by diode rectifier circuits and then connected to a multi-channel data logger. The data logger was used to record the voltage-time data.

To evaluate the amount of vibration power generation, the electric power P_i calculated by the following formula is used:

$$P_i = \frac{V_i^2}{R} \quad i = 1,2,,,,,,N \tag{10}$$

However, V_i is the voltage measurement value of the vibration power generation. R is the electrical resistance of the coil of the electromagnetic motor, and when measured directly with a tester, it was 134 ohms.

3. Results and Discussions

For a bistable vibration power generation system, there are three experimental cases: (1) random signal excitation by a general shaker, (2) periodic signal excitation by a mini-shaker, and (3) simultaneous excitation signals. Measurement experiments for the vibration response displacement and vibration power generation were conducted separately.

3.1. Excitation with Random Signal

Figure 10 shows the measurement results when only random signals were excited. The red line represents the vibration displacement of the mass block, the blue dotted line represents the vibration displacement of the support base, and the black line represents the electrical power of the vibration power generation.

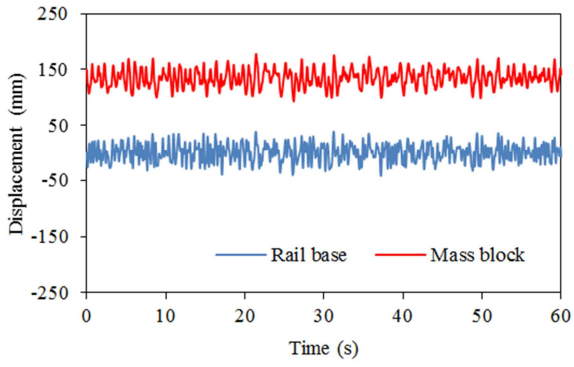

(a) Result of vibration displacement

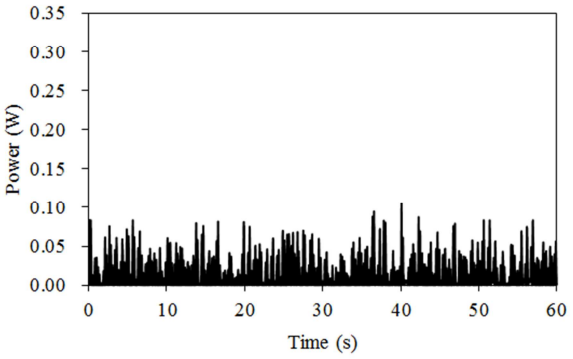

Figure 10. *Result excited by random signal.*

When excited by random signals only, the mass block vibrates mono-stably all the way to the right side of the central axis (positive side of the response displacement), which is because the mass block starts to vibrate from the right side.

The electrical power of the vibration power generation fluctuates randomly according to the amplitude change of the random vibration, and a large pick value does not appear as a whole. The maximum electrical power obtained from the vibration power generation is 105.14 mW, and the average value was 15.51 mW.

3.2. Excitation with Period Signal

Figure 11 shows the measurement results when a periodic signal of 1.0 Hz is applied. When excited at a low frequency, the vibration displacement of the mass block vibrates in almost the same phase as that of the wave-shaped rail owing to the effect of friction, and the vibration state is mono-stable. Because there is little relative displacement between the mass block and wave-shaped rail, the resulting electrical power is negligible. The maximum electrical power obtained was 2.51 mW and the average was 0.47 mW.

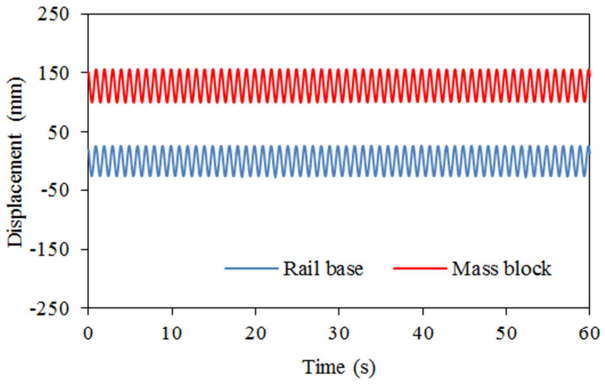

(a) Result of vibration displacement

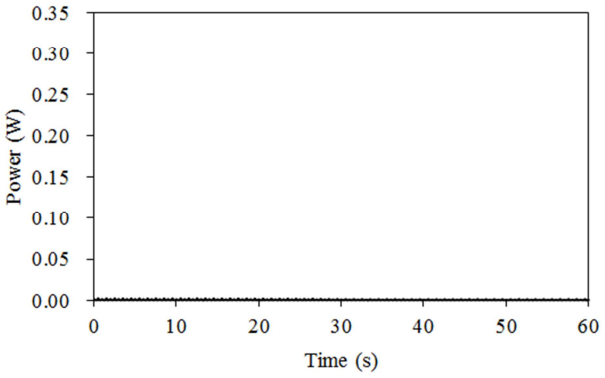

Figure 11. *Result excited by period signal 1.0 Hz.*

Figure 12 shows the measurement results when a periodic signal of 1.3 Hz is applied, and apparently there is an effect of the natural vibration mode, and the mass block vibrates slightly larger than the vibration displacement of the support. As the amplitude of the mono-stable vibration increased, the amount of power generated by the vibration power generation tended to increase. The maximum electrical power obtained was 41.70 mW and the average was 14.53 mW.

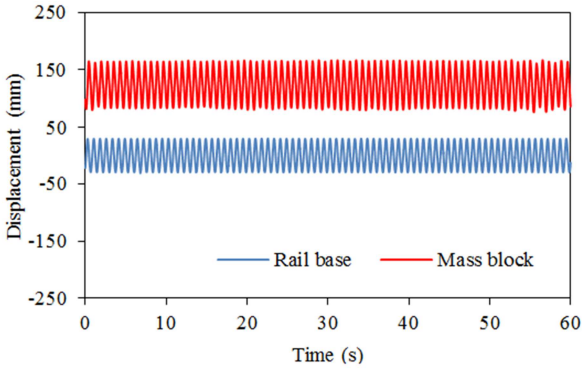

(a) Result of vibration displacement

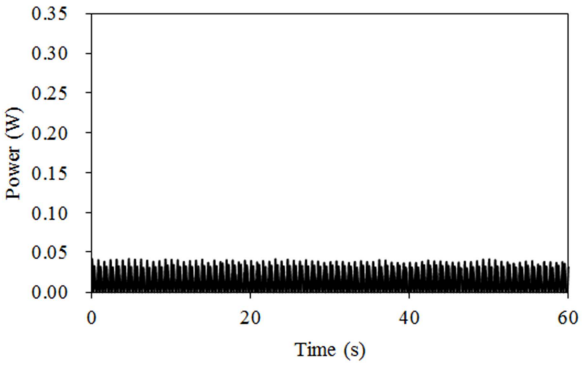

(b) Result of Electrical power

Figure 12. *Result excited by period signal 1.3 Hz.*

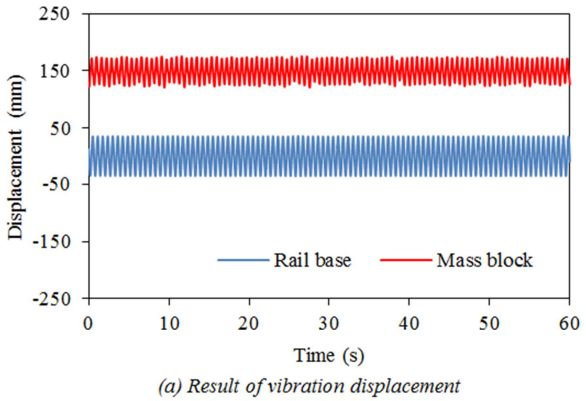

(a) Result of vibration displacement

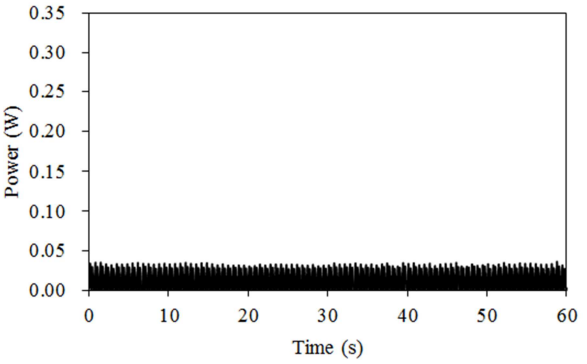

(b) Result of Electrical power

Figure 13. *Result excited by period signal 1.6 Hz.*

Figure 13 shows the measurement results for vibrations with a periodic signal of 1.6 Hz. Again, the amplitude of the mass block tended to decrease, and the mass block vibrated mono-stably to the left of the central axis. As the amplitude of the mono-stable vibration decreased, the amount of power generated by the vibration power generation tended to decrease slightly. The maximum electrical power obtained was 36.00 mW and the average was 12.78 mW.

Comparing Figure 12 and Figure 13, the amplitude when the vibration frequency is 1.3 Hz is clearly larger than that when it is 1.6 Hz; however, the difference in the obtained vibration power generation is not significant. This phenomenon is considered to be the cause of the increase in external vibration energy as the vibration frequency increases.

3.3. Excitation with Random and Period Signal

Figure 14 shows the measurement results when joint excitation was performed with a random signal and a periodic signal of 1.0 Hz. The vibration displacement of the mass block was slightly larger than that of the support, and it was in a random mono-stable vibration. As the amplitude is relatively small, the power generated by the vibration is relatively low and is distributed randomly. The maximum electrical power obtained was 154.80 mW with average of 15.88 mW.

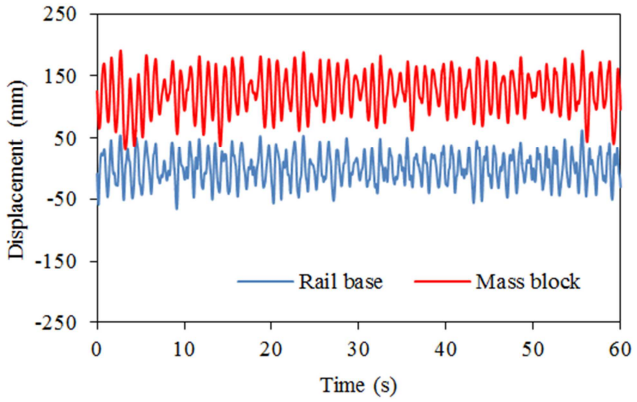

(a) Result of vibration displacement

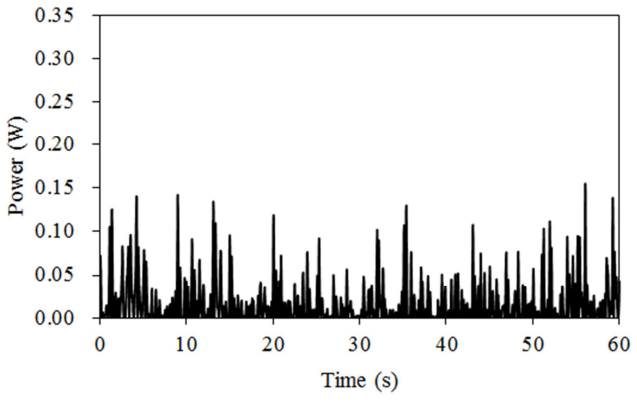

(b) Result of Electrical power

Figure 14. *Result excited by Random and period 1.0 Hz.*

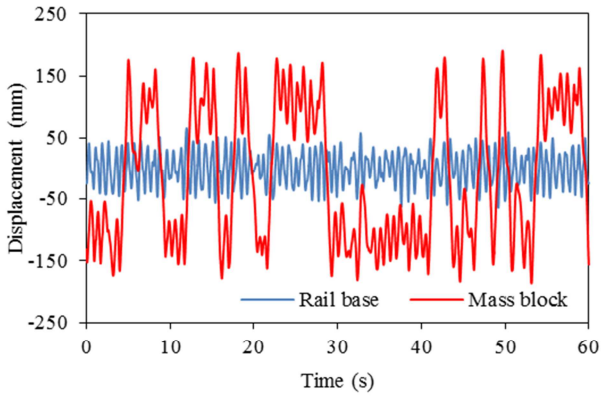

(a) Result of vibration displacement

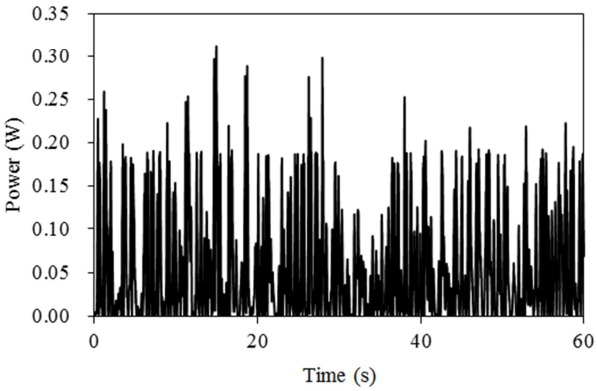

Figure 15. *Result excited by Random and period 1.3 Hz.*

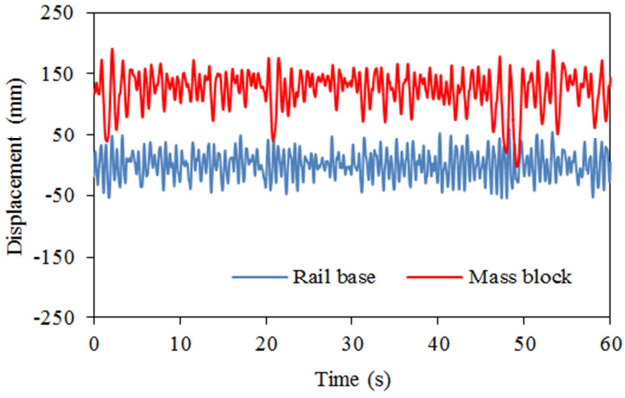

(a) Result of vibration displacement

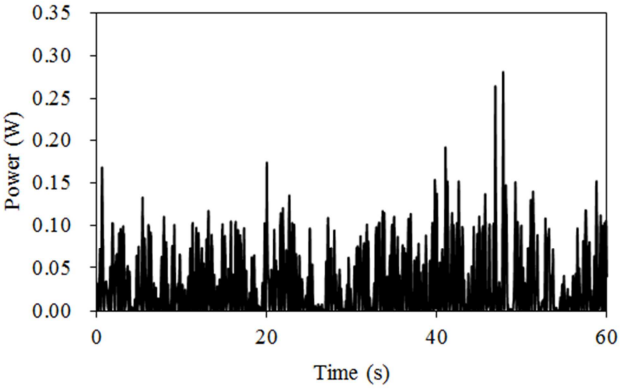

Figure 16. *Result excited by Random and period 1.6 Hz.*

Figure 15 shows the measurement results when a periodic signal of 1.3 Hz excites a random signal. The vibrations of the mass block become violent, producing bistable vibrations over the central axis, indicating that this excitation frequency region is most prone to stochastic resonance phenomena. As the amplitude at which stochastic resonance occurs increases, the amount of power generated by the vibration tends to increase. The maximum electrical power obtained was 311.55 mW with the average of 54.97 mW.

However, when the frequency of the periodic excitation signal added together with the random signal increases to 1.6 Hz, as shown in Figure 16, the vibration of the mass block conversely decreased, resulting in a monostable vibration state. As the amplitude decreased, the vibration power generation decreased slightly. The maximum electrical power obtained was 280.97 mW with average of 31.57 mW.

3.4. Amplification Effect of Stochastic Resonance

To quantitatively evaluate the amplification effect due to stochastic resonance, the standard deviation of the vibration response displacement calculated using the following equation is used:

$$S = \sqrt{\frac{1}{N}\sum_{i=1}^{N}\left(x_i - x_0\right)^2} \tag{11}$$

where x_i is the vibration displacement, x_0 is the average vibration displacement, and N is the number of vibration displacement measurements s in the time series.

Using Equation (11), the standard deviation was calculated for each measurement result of the vibration displacement obtained in the previous section, and the results are summarized in Table 1. Here, the stochastic resonance effect was evaluated using the rate of increase in the standard deviation of the vibration displacement of the mass block against the vibration displacement of the wave-shaped rail as a comparison criterion.

According to Table 1, in the random excitation, the vibration state was mono-stable, but the relative displacement between the mass block and wave-shaped rail was small, and the increase rate of the standard deviation of the vibration displacement was 0.67%.

In the periodic excitation, the relative displacement between the mass block and wave-shaped rail was larger than that in the random excitation because of the mono-stable vibration state, but the increase rate of the standard deviation of the vibration displacement remained at approximately 30%.

In joint excitation, the rate of increase of the standard deviation of the vibration displacement is clearly divided into two. In the case of excitation with periodic signals of 1.0 Hz and 1.6 Hz, the rate of increase of the standard deviation of the vibration displacement was approximately 40% because of the mono-stable vibration state. In the case of excitation with a periodic signal of 1.3 Hz, stochastic resonance phenomena associated with bistable vibration occurred, and the rate of the standard deviation of the vibration displacement increased to 306.89%.

Therefore, the amplification effect by the stochastic resonance phenomenon is significant, and the possibilities of applying it for improving the efficiency of vibration energy harvesting is indicated.

Conventional bistable vibration systems use cantilevers or elastic springs, which limit the possible range of vibration. On the other hand, the Duffing-type bistable vibration system proposed in this study has no limitation on the vibrating range of the vibrating body, and as shown in Table 1, the vibration displacement greatly increases when stochastic resonance occurs.

Table 1. *Increasing rates of the motion response displacements under different vibration states.*

Vibration signals		Mass	Base	Increasing	State
Only random		15.45	15.34	0.67%	
Periodic only	1.0 Hz	19.26	18.54	3.86%	
	1.3 Hz	28.01	21.03	33.21%	Mono-stable
	1.6 Hz	15.22	24.97	-39.01%	
Random and periodic	1.0 Hz	33.43	24.71	35.27%	
	1.3 Hz	109.87	27.00	306.89%	Bi-stable
	1.6 Hz	30.38	21.53	41.10%	Mono-stable

3.5. Power Generation Effect of Stochastic Resonance

To evaluate the efficiency of vibration power generation by stochastic resonance quantitatively, Table 2 summarizes the measurement results of the electrical power of the vibration power generation system obtained in the previous section.

Table 2. *Comparison of the amount of vibration power generation under different vibration states.*

Vibration signals		Electrical power [mW]		Vibration State
		Max	Average	
Random only		105.14	15.51	
Periodic only	1.0 Hz	2.51	0.47	
	1.3 Hz	41.70	14.53	Mono-stable
	1.6 Hz	36.00	12.78	
Random and periodic	1.0 Hz	154.80	15.88	
	1.3 Hz	311.55	54.97	Bi-stable
	1.6 Hz	280.97	31.57	Mono-stable

The results in Table 2 show that with random excitation, there is a large difference between the maximum and average values of the electrical power of the vibration power generation, indicating that vibration power generation by random excitation is unstable.

In periodic excitation, as the excitation amplitude is uniform, the difference between the maximum and average values of the electric power of the vibration power generation is relatively small, indicating that the vibration power generation by the periodic excitation is relatively stable.

In joint excitation, as in random excitation, there is a large difference between the maximum and average values of the electrical power of the vibration power generation, indicating that the vibration power generation is unstable.

However, in the case of random and periodic vibrations of 1.3 Hz, the stochastic resonance phenomenon associated with the bi-stable vibration occurred, and it was confirmed that the

amount of vibration power generation increased.

To investigate the effect of stochastic resonance on the vibration power generation efficiency, we compared the vibration power generation obtained under the same input energy conditions for the two vibration cases. One was the amount of power generated by adding the vibration power generation amounts separately obtained by excitation with random and periodic signals. The other was the vibration power generation obtained by joint excitation with two signals. The results are presented in Table 3.

Table 3. *Comparison of individual and joint excitation power generation.*

Vibration method		Average Electrical power [mW]	Vibration State
Individual excitation	1.0 Hz	15.51 + 0.47 = 15.98	Mono-stable
	1.3 Hz	15.51 + 14.53 = 30.04	
	1.6 Hz	15.51 + 12.78 = 28.29	
Joint excitation	1.0 Hz	15.88	Bi-stable
	1.3 Hz	54.97	
	1.6 Hz	31.57	Mono-stable

According to Table 3, the response vibration in the two excitation methods only has mono-stable vibration states for periodic signals of 1.0 Hz and 1.6 Hz. The difference in the average electrical power of the obtained vibration power generation was not significant.

However, in the case of a periodic signal of 1.3 Hz, the response vibration of the single excitation is mono-stable, while that of the joint excitation is bi-stable. The difference in the electrical power of vibration power generation can be calculated as follows:

$$\frac{54.97-30.04}{30.04}\times 100\% = 82.99\% \qquad (12)$$

From the result of Equation (12), it was confirmed that 82.99% more power could be generated when the two signals were excited simultaneously than when they were excited separately. However, as the external input energy is the same in the two excitation methods, the effect on the efficiency improvement of vibration power generation is very large owing to the occurrence of stochastic resonance.

Conventional bistable vibration energy harvesting systems use piezoelectric elements or simple magnets and coils, which limit the efficiency of vibration power generation. On the other hand, the Duffing-type bistable vibration energy harvesting system proposed in this research can use a power generation motor, so the vibration power generation efficiency can be relatively improved.

4. Conclusion

In this study, using the graph shape of the Duffing model, we proposed a bistable vibration energy harvesting system consisting of a new wave-shaped rail and a moving mass block and examined the characteristics of stochastic resonance and vibration power generation in detail. The following conclusions were drawn.

A new vibration energy harvesting experimental device was developed using the proposed Duffing-type bistable vibration model and an electromagnetic motor. The stochastic resonance phenomenon of the bistable vibration model was studied in detail by combining a random excitation signal that simulates the actual natural environment and a periodic excitation signal that is intentionally given. Using the bi-stable vibration model of this study, the stochastic resonance phenomenon was generated reliably, and a large amplitude expansion effect was obtained for the vibration response.

We verified the vibration power generation characteristics using the developed bi-stable vibration energy-harvesting system. A random signal simulating the natural environment and periodic signal added as a stimulus signal were used, and vibration experiments were conducted separately for two measurement cases: single excitation and joint excitation using two signals. It was confirmed that 82.99% more power was generated when the two signals were excited simultaneously under the same input excitation energy condition than when they were excited separately. From this comparison, it was found that the stochastic resonance had a significant effect on improving the efficiency of vibration power generation.

A nonlinear equation of motion for the proposed bistable vibration model was developed, and its potential energy distribution characteristics were analyzed. The Duffing bistable vibration characteristics were observed over a wide range of vibration displacements. In addition, the bistable vibration power generator developed using an electromagnetic motor can generate power stably and it can be applied for practical development of vibration energy harvesting in the future.

As a future task, we plan to develop a Duffing-type bistable vibration energy harvesting system that can actually be used in a random vibration environment in the natural world, based on the research results of this study.

References

[1] Zhang, H., Corr, L. R., & Ma, T. (2018). Issues in vibration energy harvesting. Journal of Sound and Vibration, 421, 79-90. doi.org/10.1016/j.jsv.2018.01.057.

[2] Mohanty, A., Parida, S., Behera, R. K., & Roy, T.. (2019). Vibration energy harvesting: A review. Journal of Advanced Dielectrics, 9, 4. doi.org/10.1142/S2010135X19300019.

[3] Tang, L., Yang, Y., & Soh, C. K. (2010). Toward Broadband Vibration-based Energy Harvesting. Journal of Intelligent Material Systems and Structures, 21, 18. doi.org/10.1177/1045389X10390249.

[4] Roundy, S. (2005). On the Effectiveness of Vibration-based Energy Harvesting. Journal of Intelligent Material Systems and Structures, 16, 10. doi.org/10.1177/1045389X05054042.

[5] Moss, S. D., Payne, O. R., Hart, G. A., & Ung, C. (2015). Scaling and power density metrics of electromagnetic vibration energy harvesting devices. Smart Materials and Structures, 24, 023001. doi: 10.1088/0964-1726/24/2/023001.

[6] Shahbazi, Y. (2019). Smart Flat Membrane Sheet Vibration-Based Energy Harvesters. Journal of Solid Mechanics, 11, 1, 78-90. doi: 10.22034/JSM.2019.664219.

[7] Lallart, M., Anton, S. R., & Inman, D. J. (2010). Frequency Self-tuning Scheme for Broadband Vibration Energy Harvesting. Journal of Intelligent Material Systems and Structures, 21, 9. doi.org/10.1177/1045389X10369716.

[8] Kubba, A. E., & Jiang, K. (2014). Efficiency Enhancement of a Cantilever-Based Vibration Energy Harvester. Sensors, 14, 188-211. doi: 10.3390/s140100188.

[9] Dong, L., Grissom, M., & Fisher, F. T. (2015). Resonant frequency of mass-loaded membranes for vibration energy harvesting applications. Energy, 3, 3, 344-359. doi: 10.3934/energy.2015.3.344.

[10] Dai, X. (2016). An vibration energy harvester with broadband and frequency-doubling characteristics based on rotary pendulums. Sensors and Actuators A: Physical, 241, 161-168. doi.org/10.1016/j.sna.2016.02.004.

[11] Tao, K., Ding, G., Wang, P., Liu, Q., & Yang, Z. (2012). Design and Simulation of Fully Integrated Micro Electromagnetic Vibration Energy Harvester. Applied Mechanics and Materials, 152-154, 1087-1090. doi.org/10.4028/www.scientific.net/AMM.152-154.1087.

[12] Zayed, A. A. A., Assal, S. F. M., Nakano, K., Kaizuka, T., & El-Bab, A. M. R. F. (2019). Design Procedure and Experimental Verification of a Broadband Quad-Stable 2-DOF Vibration Energy Harvester. Sensors, 19, 2893. doi.org/10.3390/s19132893.

[13] Ramlan, R., Brennan, M. J., Mace, B. R., & Burrow, S. G. (2012). On the performance of a dual-mode non-linear vibration energy harvesting device. Journal of Intelligent Material Systems and Structures, 23 (13), 1423-1432. doi: 10.1177/1045389X12443017.

[14] Gammaitoni, L., Neri, I., & Vocca, H. (2009). Nonlinear oscillators for vibration energy harvesting. Applied Physics Letters, 94, 164102. doi: 10.1063/1.3120279.

[15] Gafforelli, G., Corigliano, A., Xu, R., & Kim, S. G. (2014). Experimental verification of a bridge-shaped, nonlinear vibration energy harvester. Applied Physics Letters, 105, 203901. doi: 10.1063/1.4902116.

[16] Liu, W. Q., Badel, A., Formosa, F., & Wu, Y. P. (2015). A new figure of merit for wideband vibration energy harvesters. Smart Materials and Structures, 24, 12. doi: 10.1088/0964-1726/24/12/125012.

[17] Yang, W., & Towfighian, S. (2017). A hybrid nonlinear vibration energy harvester. Mechanical Systems and Signal Processing, 90, 317-333. doi.org/10.1016/j.ymssp.2016.12.032.

[18] Kumar, A., Ali, S. F., & Arockiarajan, A. (2018). Exploring the benefits of an asymmetric monostable potential function in broadband vibration energy harvesting. Applied Physics Letters, 112, 233901. doi: 10.1063/1.5037733.

[19] Su, D., Nakano, K., Zheng, R., & Cartmell, M. P. (2014). Investigations of a Stiffness Tunable Nonlinear Vibrational Energy Harvester. International Journal of Structural Stability and Dynamics, 14, 8. doi: 10.1142/S0219455414400239.

[20] Zhang, G., & Hu, J. (2014). A Branched Beam-Based Vibration Energy Harvester. Journal of Electronic Materials, 43, 3912-3921. doi: 10.1007/s11664-014-3398-5.

[21] Zhou, S., Chen, W., Malakooti, D. H., Cao, J., & Inman, D. J. (2016). Design and modeling of a flexible longitudinal zigzag structure for enhanced vibration energy harvesting. Journal of Intelligent Material Systems and Structures, 1, 14. doi: 10.1177/1045389X16645862.

[22] Lee, H., Sharpes, N., Abdelmoula, H., Abdelkefi, A., & Priya, S. (2018). Higher power generation from torsion-dominant mode in a zigzag shaped two-dimensional energy harvester, Applied Energy, 216, 494-503. doi.org/10.1016/j.apenergy.2018.02.083.

[23] Sharpes, N., Abdelkefi, A., Abdelmoula, H., Kumar, P., Adler, J., & Priya, S. (2016). Mode shape combination in a two-dimensional vibration energy harvester through mass loading structural modification. Applied Physics Letters, 109, 033901. doi.org/10.1063/1.4958689.

[24] Ansari, M. H. & Karami, M. A. (2016). Modeling and experimental verification of a fan-folded vibration energy harvester for leadless pacemakers, Journal of Applied Physics, 119, 094506. doi.org/10.1063/1.4942882.

[25] Malaji, P. V., & Ali, S. F. (2017). Magneto-mechanically coupled electromagnetic harvesters for broadband energy harvesting. Applied Physics Letters, 111, 083901. doi.org/10.1063/1.4997297.

[26] Jiang, W. A., & Chen, L. Q. (2016). Stochastic averaging of energy harvesting systems. International Journal of Non-Linear Mechanics, 85, 174-187. doi.org/10.1016/j.ijnonlinmec.2016.07.002.

[27] Dykman, M. I., Luchinsky, D. G., Mannella, R., McClintock, P. V. E., Stein, N. D. & Stocks, N. G. (1993). Nonconventional Stochastic Resonance. Journal of Statistical Physics, 70, 479-499. doi.org/10.1007/BF01053983.

[28] Gammaitoni, L. (1999). Stochastic resonance. Review of Modern Physics, 70, 223. doi.org/10.1103/RevModPhys.70.223.

[29] Harne, R. L., & Wang, K. W. (2013). A review of the recent research on vibration energy harvesting via bistable systems. Smart Materials and Structures, 22, 2, 023001. doi: 10.1088/0964-1726/22/2/023001.

[30] Pellegrini, S. P., Tolou, N., Schenk, M., & Herder, J. L. (2013). Bistable vibration energy harvesters: A review. Journal of Intelligent Material Systems and Structures, 24 (11) 1303-1312. doi: 10.1177/1045389X12444940.

[31] Zheng, R., Nakano, K., Hu, H., Su, D., & Cartmell, M. P. (2014). An application of stochastic resonance for energy harvesting in a bistable vibrating system. Journal of Sound and Vibration, 333, 2568-2587. doi.org/10.1016/j.jsv.2014.01.020

[32] Wang, K., Dai, X., Xiang, X., Ding, G., & Zhao, X. (2019). Optimal potential well for maximizing performance of bi-stable energy harvester. Applied Physics Letters, 115, 143904. doi: 10.1063/1.5095693.

[33] Ibrahim, A., Towfighian, S., & Younis, M. I. (2017). Dynamics of Transition Regime in Bistable Vibration Energy Harvesters. Journal of Vibration and Acoustics, 139, 051008. doi: 10.1115/1.4036503.

[34] Kumar, A., Sharma, A., Vaish, R., Kumar, R., & Jain, S. C. (2018). A numerical study on flexoelectric bistable energy harvester. Applied Physics A, 124, 483. doi.org/10.1007/s00339-018-1889-6

[35] Leng, Y. G., Gao, Y. J., Tan, D., Fan, S. B., & Lai, Z. H. (2015). An elastic-support model for enhanced bistable piezoelectric energy harvesting from random vibrations. Journal of Applied Physics, 117, 064901. doi: 10.1063/1.4907763.

[36] Friswell, M. I., Ali, S. F., Bilgen, O., Adhikari, S., Lees, A. W., & Litak, G. (2012). Non-linear piezoelectric vibration energy harvesting from a vertical cantilever beam with tip mass. Journal of Intelligent Material Systems and Structures, 23 (13), 1505-1521. doi: 10.1177/1045389X12455722.

[37] Bilgen, O., Friswell, M. I., Ali, S. F., & Litak, G. (2015). Broadband Vibration Energy Harvesting from a Vertical Cantilever Piezocomposite Beam with Tip Mass. International Journal of Structural Stability and Dynamics, 15, 2, 1450038. doi: 10.1142/S0219455414500382.

[38] Lan, C. B., & Qin, W. Y. (2014). Energy harvesting from coherent resonance of horizontal vibration of beam excited by vertical base motion. Applied Physics Letters, 105, 113901. doi: 10.1063/1.4895921.

[39] Zhao, W., Wu, Q., Zhao, X., Nakano, K., & Zheng, R. (2020). Development of large-scale bistable motion system for energy harvesting by application of stochastic resonance. Journal of Sound and Vibration, 473, 115213. doi.org/10.1016/j.jsv.2020.115213.

[40] Guo, L., Zhao, W., Gomi, N., Guan, J., & Zhao, X. (2022). Development of an Opposed Mass-Spring Type Bi-Stable Vibration Energy Harvesting System Using Stochastic Resonance. International Journal of Mechanical Engineering and Applications, 10 (6): 123-134. doi: 10.11648/j.ijmea.20221006.11.

[41] Zhao, W., Zheng, R., Yin, X., Zhao, X., & Kimihiko, K. (2021). An Electromagnetic Energy Harvester of Large-Scale Bistable Motion by Application of Stochastic Resonance. Journal of Vibration and Acoustics, 144, 011007. doi: 10.1115/1.4051265.

[42] Guo, L., Zhao, W., Guan, J., Gomi, N., & Zhao, X. (2022). Horizontal Bi-Stable Vibration Energy Harvesting Using Electromagnetic Induction and Power Generation Efficiency Improvement via Stochastic Resonance. Machines, 10, 899. doi.org/10.3390/machines10100899.